

Supplement of

Non-linear Climatic Response to the Weakening of the Atlantic Meridional Overturning Circulation During Glacial Times

5 **Yanxuan Du, Josephine R. Brown, Lauire Menviel, Himadri Saini, Russell N. Drysdale, David K. Hutchinson, and Calla N. Gould-Whaley**

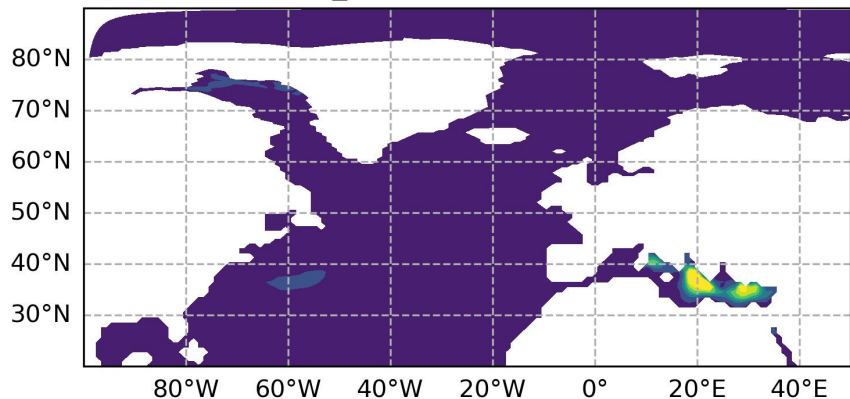
Correspondence to: Yanxuan Du (yanxuand@student.unimelb.edu.au)

10

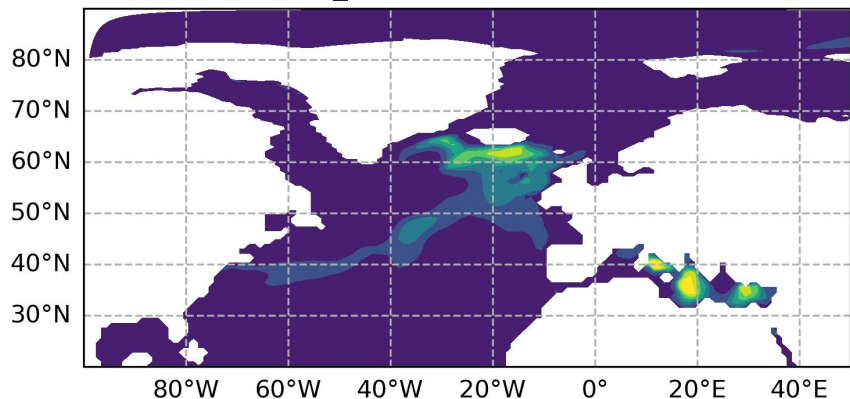
15

20

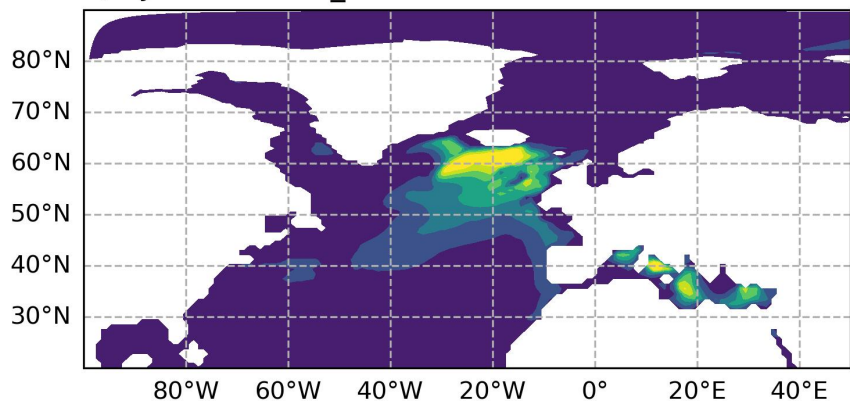
a) DJF MLD: 49ka_shutdown



b) DJF MLD: 49ka_0.3Sv



c) DJF MLD: 49ka_0.2Sv



25 **Figure S1:** Full field mixed layer depth (MLD; in m) in the North Atlantic in DJF season for Heinrich stadial (a) 49ka_shutdown, and D-O stadial simulations (b) 49ka_0.3Sv, (c) 49ka_0.2Sv.

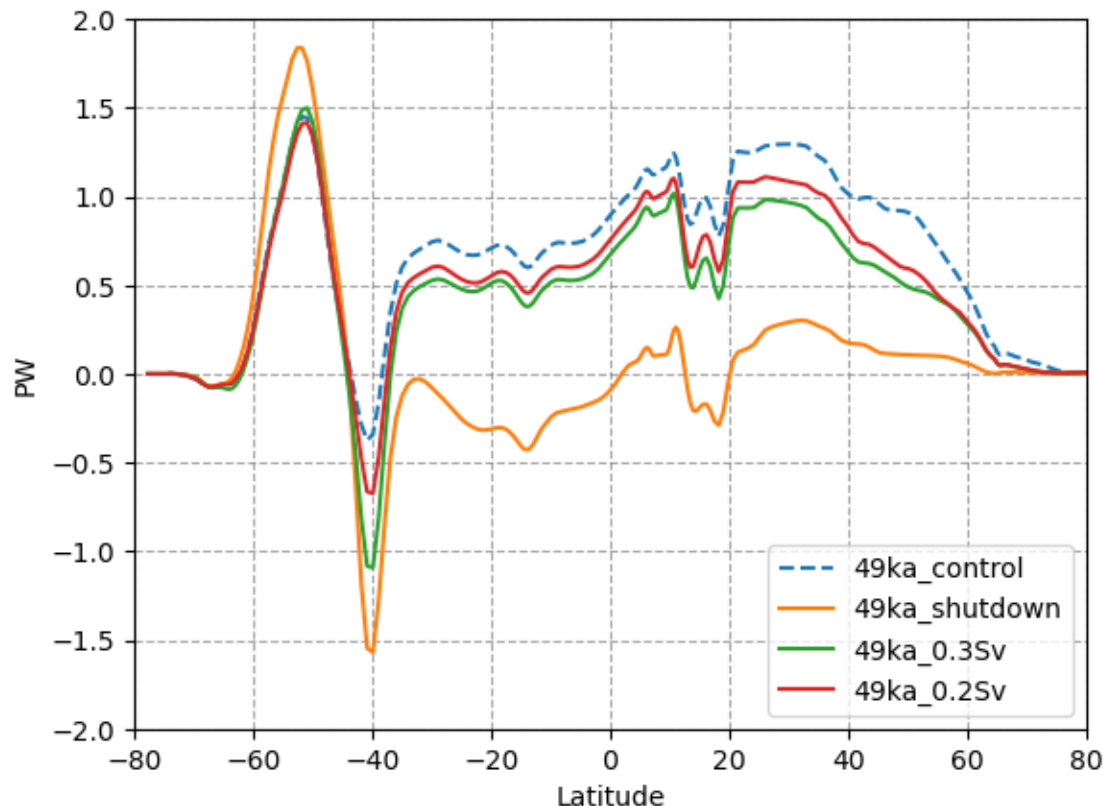
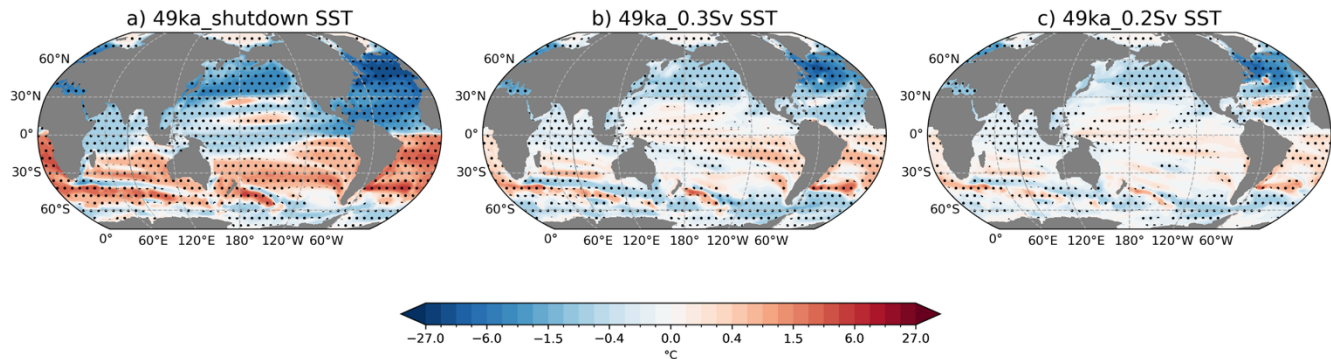


Figure S2: Meridional oceanic heat transport (PW) over the Atlantic Ocean in 49ka_control, 49ka_shutdown, 49ka_0.3Sv and 49ka_0.2Sv simulations.

30

35



40 **Figure S3:** Annual sea surface temperature anomalies (SST; °C) relative to 49ka_control in each simulation. Stippling indicates statistically
significance differences from the control at the 95 % confidence level according to the Student's t-test.

45

50

55

60

65

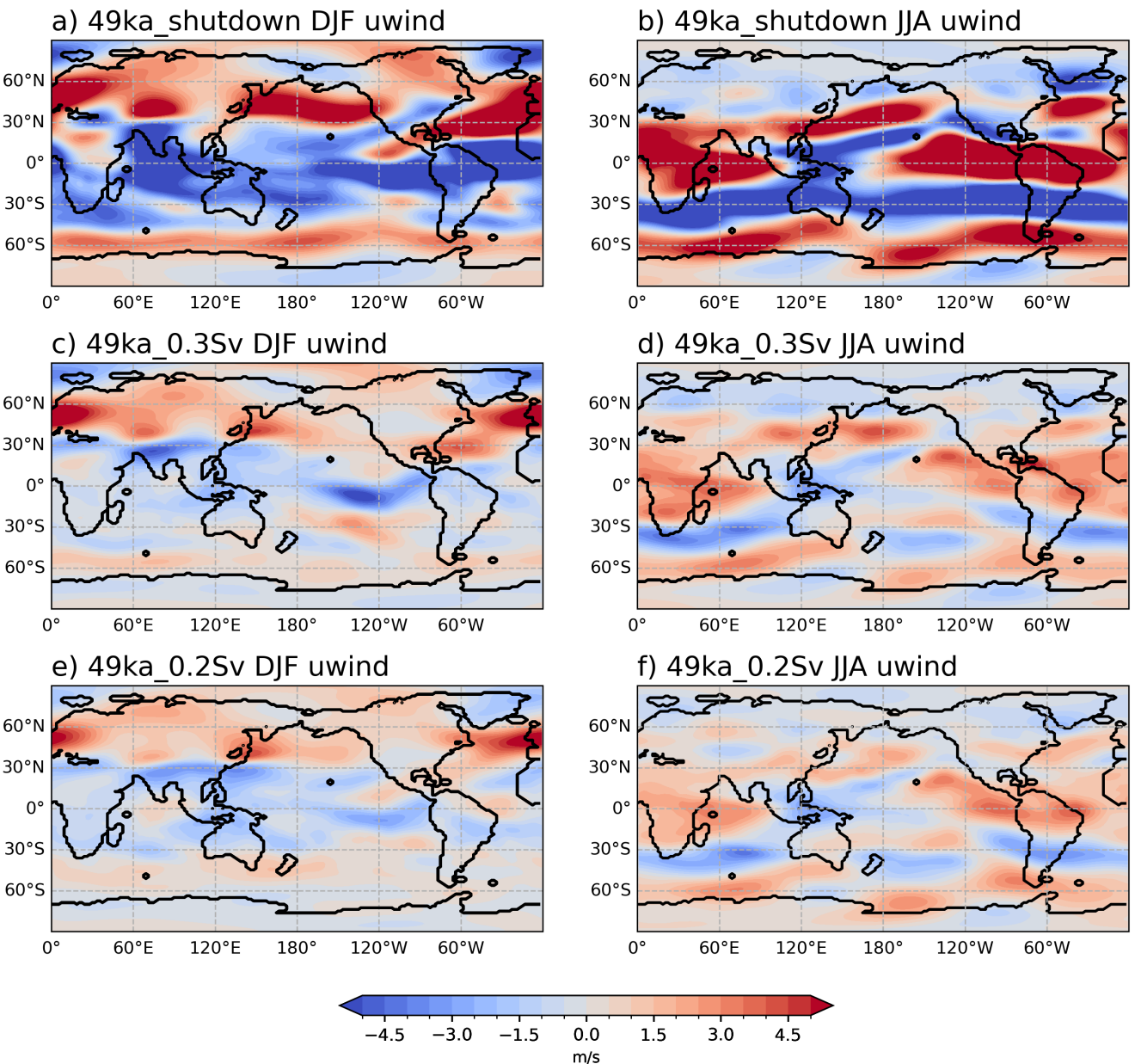
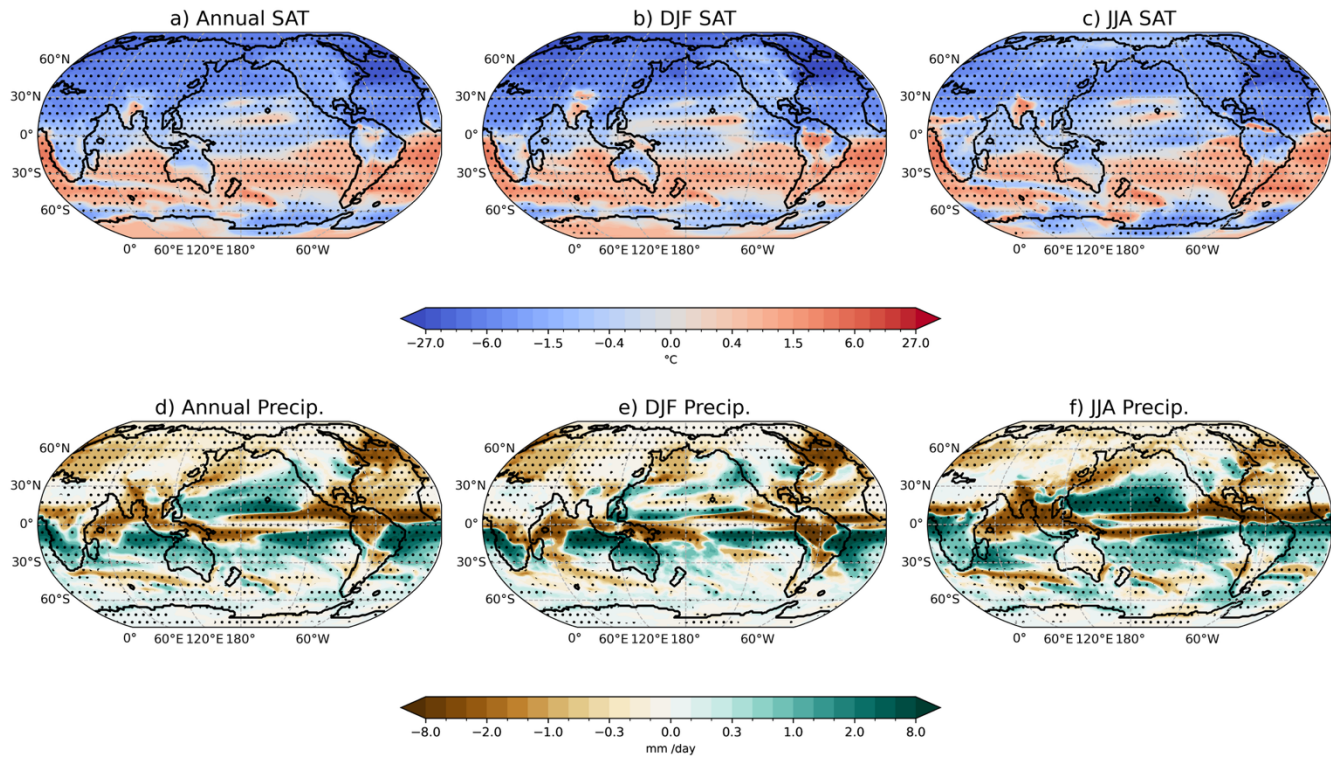


Figure S4: DJF and JJA 200 hPa zonal wind speed anomalies (m/s) relative to 49ka_control in each simulation.



75 **Figure S5:** 49ka_shutdown annual, DJF and JJA surface air temperature anomalies (SAT; °C), and precipitation anomalies (mm/day) relative to 49ka_control. Stippling indicates statically significant differences from the control at the 95 % level according to the Student's t-test.

80

85

90

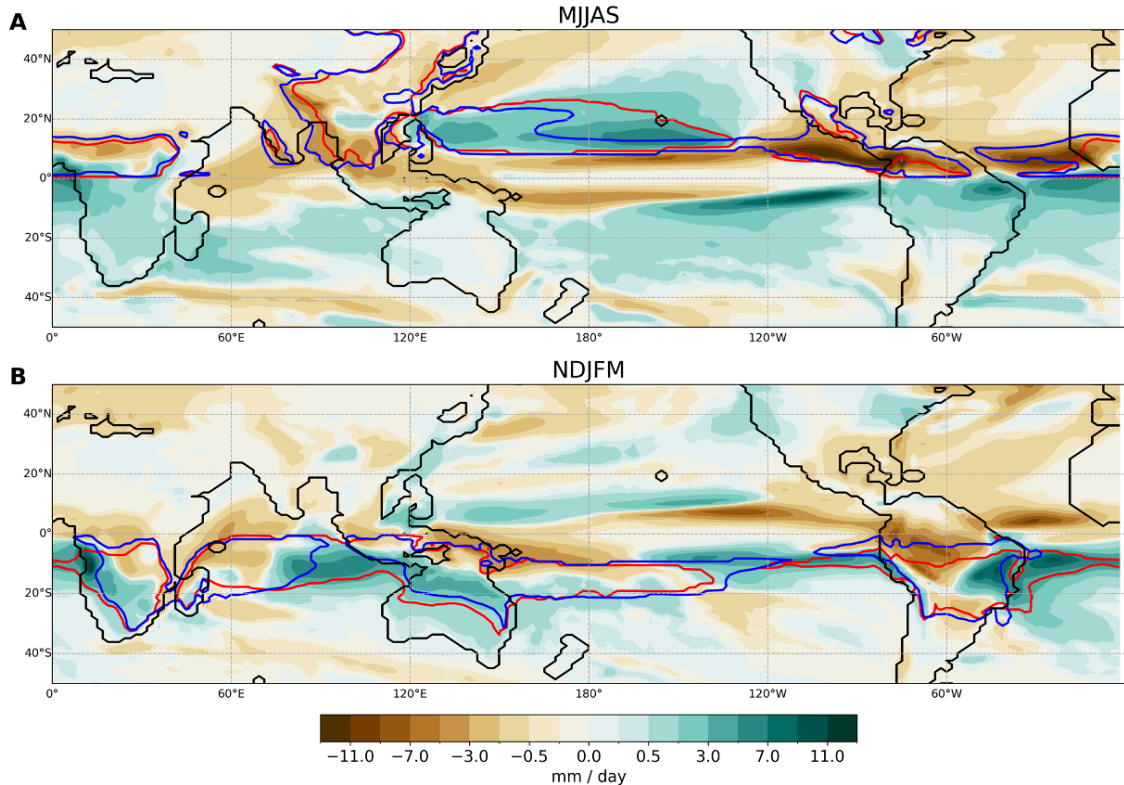


Figure S6: 49ka_shutdown (Heinrich stadial) – 49ka_control precipitation anomaly (mm/day) and monsoon domains in (a) Northern Hemisphere monsoon season: MJIAS, and (b) Southern Hemisphere monsoon season: NDJFM. Contours indicate monsoon domains for Heinrich stadial (in red) and for control (in blue) experiments.

95

100

105

Table S1. Area-weighted normalized annual mean surface air temperature (SAT) and precipitation anomalies per 1 Sv

110 AMOC decrease in each experiment relative to 49ka_control. This includes global, NH, SH (0-55° S) temperature changes,
and global, NH, and SH (0-90° S) precipitation changes.

| Experiment | Global SAT (°C/Sv) | NH SAT (°C/Sv) | SH SAT (0-55° S) (°C/Sv) | Global precip (mm day ⁻¹ /Sv) | NH precip (mm day ⁻¹ /Sv) | SH precip (mm day ⁻¹ /Sv) |
|---------------|-----------------------|-------------------|--------------------------------|---|---|---|
| 49ka_0.2Sv | -0.046 | -0.08 | -0.0023 | -0.0029 | -0.0094 | 0.0036 |
| 49ka_0.3Sv | -0.046 | -0.08 | -0.0026 | -0.0027 | -0.009 | 0.0037 |
| 49ka_shutdown | -0.061 | -0.13 | 0.015 | -0.0036 | -0.018 | 0.011 |

115

Table S2. Wintertime northern (DJF) and southern (JJA) HC mean latitudinal position (°), strength (Sv), and positions (°) of its ascending and descending branches at 500 hPa in each experiments, interpolated to 0.5° latitude resolution using the calculation methods described in Section 2.4.

120

| Experiment | Northern HC in DJF | | | | Southern HC in JJA | | | |
|---------------|--------------------|---------------|----------------------|-----------------------|--------------------|---------------|----------------------|-----------------------|
| | Mean position (°) | Strength (Sv) | Ascending branch (°) | Descending branch (°) | Mean position (°) | Strength (Sv) | Ascending branch (°) | Descending branch (°) |
| 49ka_control | 8.125 | 476.8 | -15.6 | 28.0 | -0.375 | -486.6 | 14.9 | -27.2 |
| 49ka_0.2Sv | 8.125 | 482.9 | -15.7 | 27.9 | -0.875 | -473.0 | 14.7 | -27.4 |
| 49ka_0.3Sv | 8.125 | 487.1 | -15.9 | 28.0 | -0.875 | -467.0 | 14.3 | -27.2 |
| 49ka_shutdown | -1.875 | 572.5 | -17.1 | 28.1 | -8.375 | -328.7 | 18.4 | -28.7 |